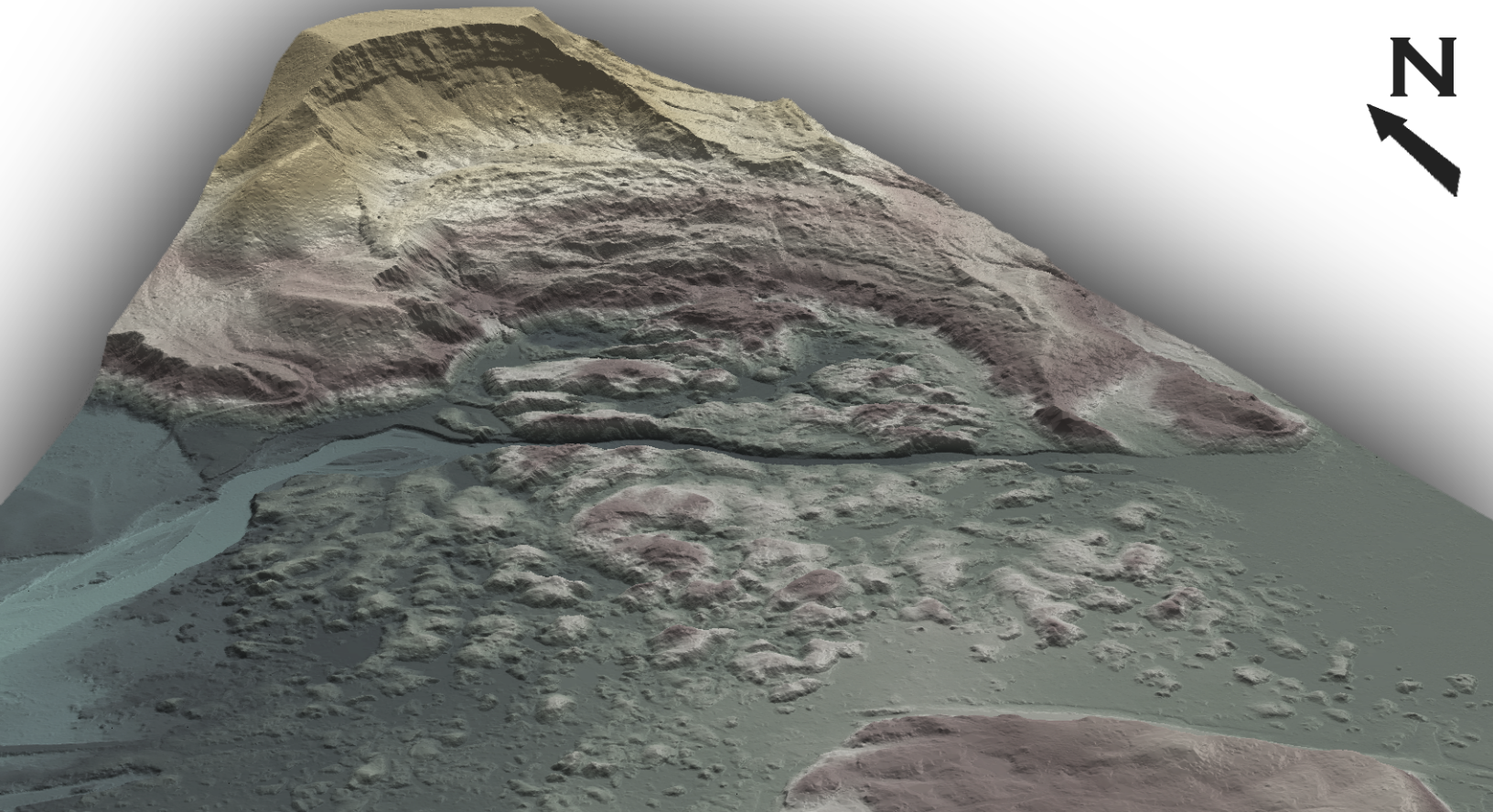


May 28, 2014



Oso Landslide/Stillaguamish River LiDAR

Technical Data Report



Scott Campbell
WSDOT
810 Maple Park Ave. SE
Olympia WA. 98504
PH: 360-596-8945



QSI Corvallis Office
517 SW 2nd St., Suite 400
Corvallis, OR 97333
PH: 541-752-1204

TABLE OF CONTENTS

| | |
|----------------------------------------|----|
| INTRODUCTION | 1 |
| Deliverable Products | 2 |
| ACQUISITION | 4 |
| Planning..... | 4 |
| Ground Control..... | 5 |
| Monumentation | 5 |
| Ground Survey Points (GSP) | 6 |
| Airborne Survey..... | 8 |
| LiDAR..... | 8 |
| PROCESSING | 9 |
| LiDAR Data..... | 9 |
| RESULTS & DISCUSSION..... | 11 |
| LiDAR Density | 11 |
| LiDAR Accuracy Assessments | 14 |
| LiDAR Absolute Accuracy..... | 14 |
| LiDAR Vertical Relative Accuracy | 15 |
| CERTIFICATIONS | 17 |
| SELECTED IMAGES..... | 18 |
| GLOSSARY | 26 |
| APPENDIX A - ACCURACY CONTROLS | 27 |

Cover Photo: A view looking over the Oso landslide. The gridded bare earth model is colored by elevation.

INTRODUCTION

This photo taken by QSI acquisition staff shows a view of the Oso Landslide site in Washington.



In March 2014, Quantum Spatial (QSI) was contracted by the Washington State Department of Transportation (WSDOT) to collect Light Detection and Ranging (LiDAR) data as soon as possible of the March 22nd, 2014 Oso Landslide disaster site. Initial LiDAR data were acquired on Monday, March 24th to aid WSDOT in their emergency response to the landslide. The landslide area was re-acquired in early April, as part of an expanded LiDAR project area that includes the Stillaguamish River drainage.

This report accompanies the delivered LiDAR data, and documents contract specifications, data acquisition procedures, processing methods, and analysis of the final dataset including LiDAR accuracy and density. Data for the initial emergency response flight were delivered on March 28th without a separate accompanying report, and therefore details of that data are also included. Acquisition dates and acreage are shown in Table 1, a complete list of contracted deliverables provided to WSDOT is shown in Table 2, and the project extent for both data deliveries is shown in Figure 1.

Table 1: Acquisition dates, acreage, and data types collected on the Oso Landslide sites

| Project Site | Contracted Acres | Buffered Acres | Acquisition Dates | Data Type |
|--------------------------------------------------------------|------------------|----------------|------------------------------------------------------------|-----------|
| Oso Landslide – Initial Acquisition | 5,151 | 5,616 | 03/24/2014 | LiDAR |
| Oso Landslide/ Stillaguamish River – Final Acquisition | 36,932 | 39,725 | 04/02 – 04/03, 2014; 04/06 – 04/07, 2014; 04/09/2014 | LiDAR |

Deliverable Products

Table 2: Products delivered to WSDOT for the Oso Landslide/Stillaguamish River site

| Oso Landslide/Stillaguamish River Products Projection: Washington State Plane North Horizontal Datum: NAD83 (2011) Vertical Datum: NAVD88 (GEOID12A) Units: US Survey Feet | |
|---------------------------------------------------------------------------------------------------------------------------------------------------------------------------------------------------------------------------|--------------------------------------------------------------------------------------------------------------------------------------------------------------------------------------------------------------|
| Points | LAS v 1.2 <ul style="list-style-type: none"> • All Returns Comma Delimited ASCII Files (*.asc) <ul style="list-style-type: none"> • All Returns • Ground Returns |
| Rasters | 3.0 Foot ESRI Grids <ul style="list-style-type: none"> • Bare Earth Model • Highest Hit Model 1.5 Foot GeoTiffs <ul style="list-style-type: none"> • Intensity Images |
| Vectors | Shapefiles (*.shp) <ul style="list-style-type: none"> • Site Boundary • LiDAR Tile Index • DEM Tile Index • Smooth Best Estimate Trajectory (SBETs) |

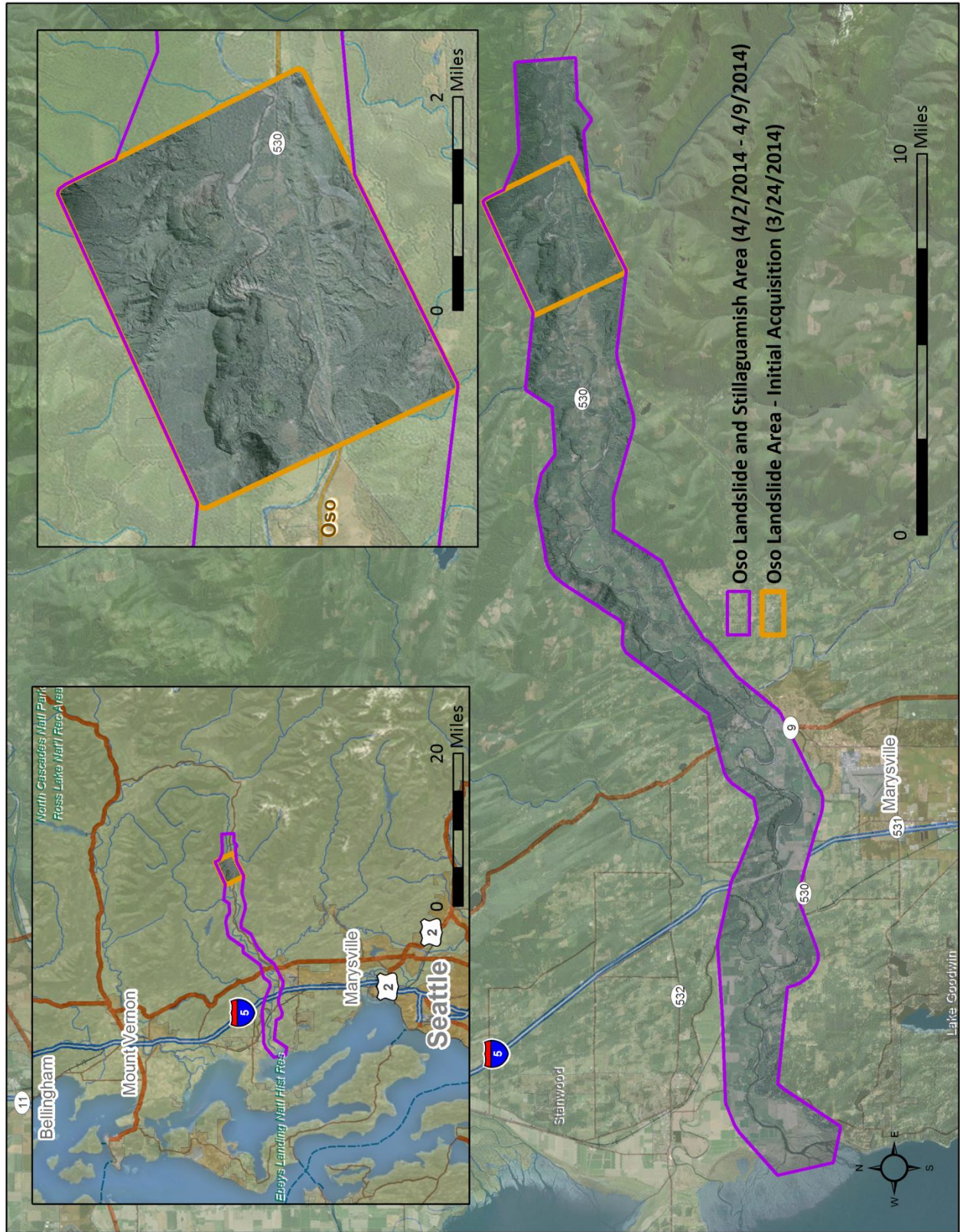


Figure 1: Location map of the Oso Landslide/Stillaguamish River site in Washington

QSI's ground acquisition equipment set up in the Oso Landslide/Stillaguamish River LiDAR study area.



Planning

In preparation for data collection, QSI reviewed the project area and developed a specialized flight plan to ensure complete coverage of the Oso Landslide/Stillaguamish River LiDAR study area at the target point density of ≥ 8.0 points/m² (0.74 points/ft²). Acquisition parameters including orientation relative to terrain, flight altitude, pulse rate, scan angle, and ground speed were adapted in order to optimize flight paths and flight times while meeting all contract specifications.

Factors such as satellite constellation availability and weather windows must be considered during the planning stage. Any weather hazards or conditions affecting the flight were continuously monitored due to their potential impact on the daily success of airborne and ground operations. In addition, logistical considerations including private property access and potential air space restrictions were reviewed.

Ground Control

Ground control surveys, including monumentation and ground survey points (GSP), were conducted to support the airborne acquisition process. Ground control data were used to geospatially correct the aircraft positional coordinate data and to perform quality assurance checks on final LiDAR data.



WSDOT Monument

Monumentation

The spatial configuration of ground survey monuments provided redundant control within 13 nautical miles of the mission areas for LiDAR flights. Monuments were also used for collection of ground survey points using real time kinematic (RTK) and post processed kinematic (PPK) survey techniques.

Monument locations were selected with consideration for satellite visibility, field crew safety, and optimal location for GSP coverage. QSI utilized two existing WSDOT monuments and established three new monuments for the Oso Landslide/Stillaguamish River LiDAR project (Table 3, Figure 2). New monumentation was set using 5/8" x 30" rebar topped with stamped 2" aluminum caps. QSI's professional land surveyor Chris Brown (WA PLS# 46328 LS) oversaw and certified the establishment of all monuments.

Table 3: Monuments established for the Oso Landslide/Stillaguamish River acquisition. Coordinates are on the NAD83 (2011) datum, epoch 2010.00

| Monument ID | Latitude | Longitude | Ellipsoid (meters) |
|-------------|-------------------|---------------------|--------------------|
| OM_1 | 48° 16' 25.06654" | -121° 59' 24.27193" | 20.659 |
| OM_2 | 48° 12' 42.89637" | -122° 20' 20.81099" | -18.007 |
| OM_3 | 48° 14' 31.41124" | -122° 03' 32.24476" | 7.763 |
| WSDOT_1627 | 48° 16' 20.02142" | -121° 54' 02.74581" | 53.448 |
| WSDOT_958 | 48° 11' 19.33409" | -122° 10' 42.89980" | -6.113 |

To correct the continuously recorded onboard measurements of the aircraft position, QSI concurrently conducted multiple static Global Navigation Satellite System (GNSS) ground surveys (1 Hz recording frequency) over each monument. During post-processing, the static GPS data were triangulated with nearby Continuously Operating Reference Stations (CORS) using the Online Positioning User Service (OPUS¹) for precise positioning. Multiple independent sessions over the same monument were processed to confirm antenna height measurements and to refine position accuracy.

Monuments were established according to the national standard for geodetic control networks, as specified in the Federal Geographic Data Committee (FGDC) Geospatial Positioning Accuracy Standards

¹ OPUS is a free service provided by the National Geodetic Survey to process corrected monument positions. <http://www.ngs.noaa.gov/OPUS>.

for geodetic networks.² This standard provides guidelines for classification of monument quality at the 95% confidence interval as a basis for comparing the quality of one control network to another. The monument rating for this project is shown in Table 4.

Table 4: Federal Geographic Data Committee monument rating for network accuracy

| Direction | Rating |
|-------------------------------|---------|
| 1.96 * St Dev _{NE} : | 0.020 m |
| 1.96 * St Dev _z : | 0.050 m |

For the Oso Landslide/Stillaguamish River LiDAR project, the monument coordinates contributed no more than 5.4 cm of positional error to the geolocation of the final GSP and LiDAR, with 95% confidence.

Ground Survey Points (GSP)

Ground survey points were collected using real time kinematic (RTK) and post-processed kinematic (PPK) survey techniques. For RTK, a Trimble R7 receiver was positioned at a nearby monument to broadcast a kinematic correction to a roving Trimble R8 GNSS receiver. For PPK, these corrections were applied during post-processing. All GSP measurements were made during periods with a Position Dilution of Precision (PDOP) of ≤ 3.0 with at least six satellites in view of the stationary and roving receivers. When collecting RTK and PPK data, the rover records data while stationary for five seconds, then calculates the pseudorange position using at least three one-second epochs. Relative errors for the position must be less than 1.5 cm horizontal and 2.0 cm vertical in order to be accepted. See Table 5 for Trimble unit specifications.

GSP were collected in areas where good satellite visibility was achieved on paved roads and other hard surfaces such as gravel or packed dirt roads. GSP measurements were not taken on highly reflective surfaces such as center line stripes or lane markings on roads due to the increased noise seen in the laser returns over these surfaces. GSP were collected within as many flightlines as possible, however the distribution of GSP depended on ground access constraints and monument locations and may not be equitably distributed throughout the study area (Figure 2).

Table 5: Trimble equipment identification

| Receiver Model | Antenna | OPUS Antenna ID | Use |
|-----------------|-----------------------------------|-----------------|---------------|
| Trimble R7 GNSS | Zephyr GNSS Geodetic Model 2 RoHS | TRM57971.00 | Static |
| Trimble R8 | Integrated Antenna R8 Model 2 | TRM_R8_GNSS | Static, Rover |

² Federal Geographic Data Committee, Geospatial Positioning Accuracy Standards (FGDC-STD-007.2-1998). Part 2: Standards for Geodetic Networks, Table 2.1, page 2-3. <http://www.fgdc.gov/standards/projects/FGDC-standards-projects/accuracy/part2/chapter2>

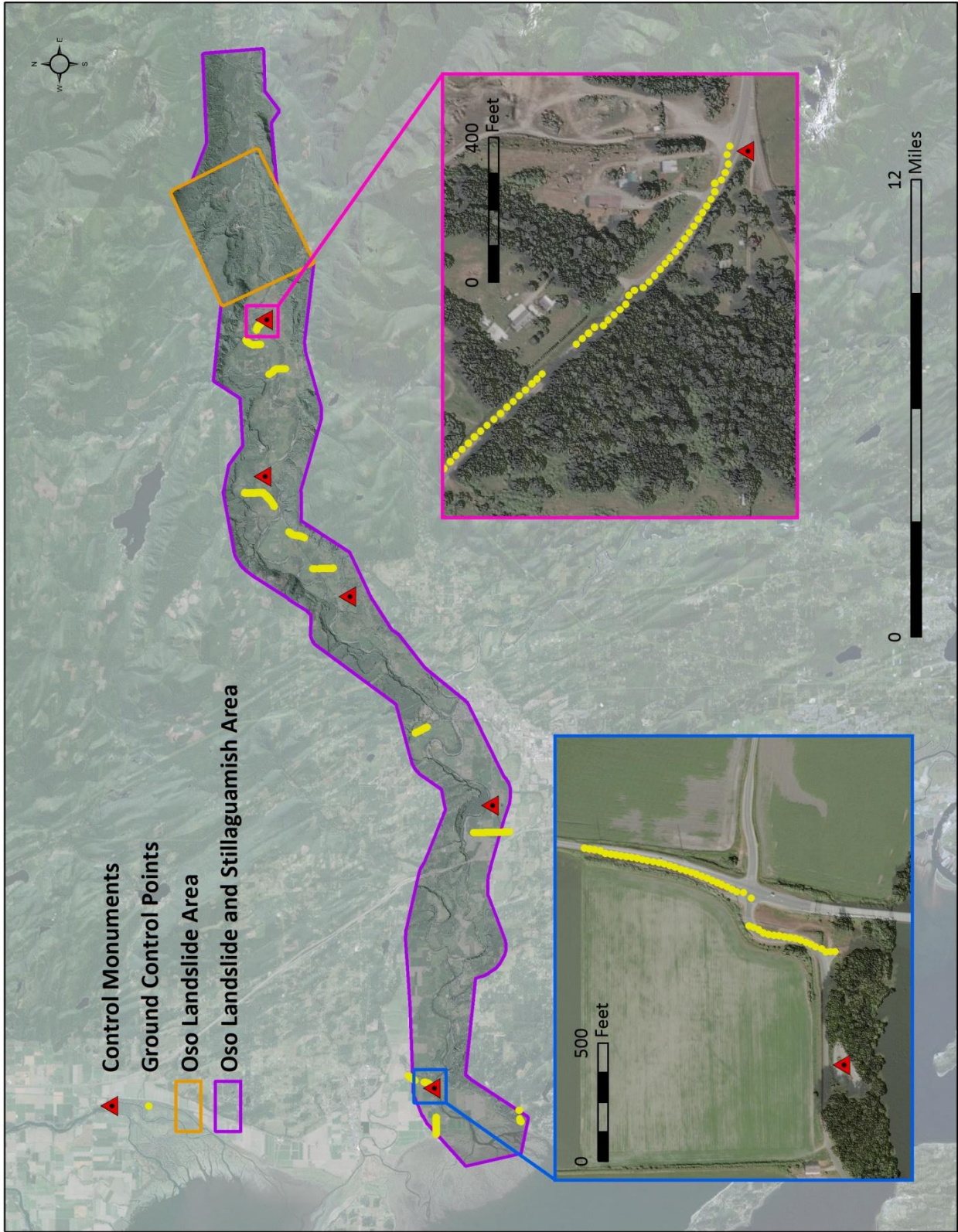


Figure 2: Ground control location map

Airborne Survey

LiDAR

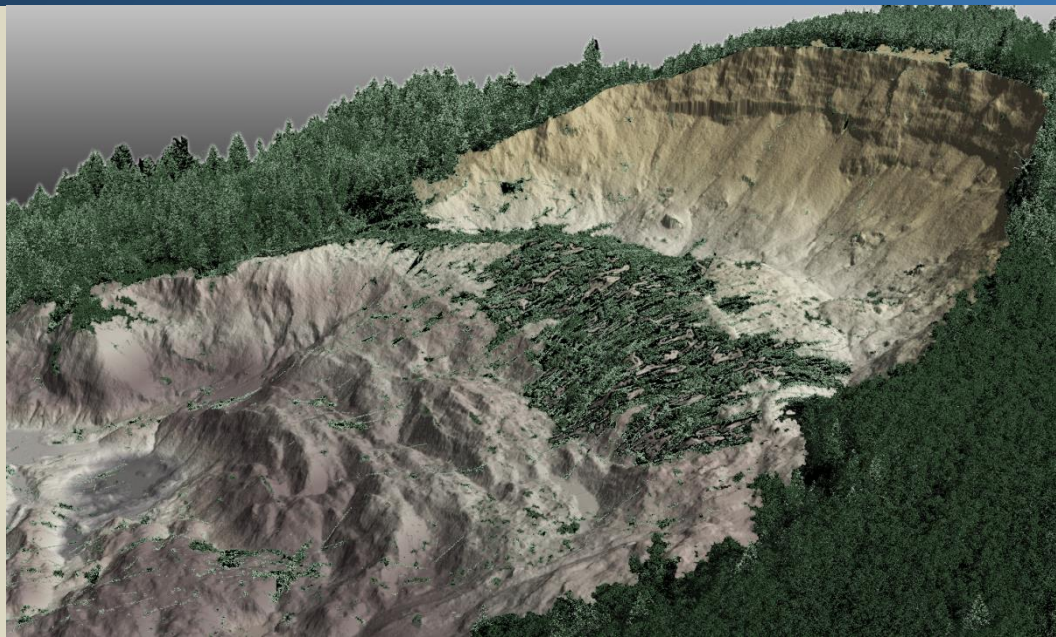
The LiDAR survey was accomplished using a Leica ALS50 Phase II system mounted in a Cessna 206. Table 6 summarizes the settings used to yield an average pulse density of ≥ 8 pulses/m² over the Oso Landslide/Stillaguamish River project area. The Leica laser system records up to four range measurements (returns) per pulse. It is not uncommon for some types of surfaces (e.g., dense vegetation or water) to return fewer pulses to the LiDAR sensor than the laser originally emitted. The discrepancy between first return and delivered density will vary depending on terrain, land cover, and the prevalence of water bodies. All discernible laser returns were processed for the output dataset.

Table 6: LiDAR specifications and survey settings

| LiDAR Survey Settings & Specifications | | |
|----------------------------------------|-------------------------------------------------------------------------|---------------------------------|
| Acquisition Dates | March 24, 2014, April 2 – 3, 2014, April 6 – 7, 2014, and April 9, 2014 | April 9, 2014 |
| Aircraft Used | Cessna 206 | Cessna 206 |
| Sensor | Leica ALS50 | Leica ALS50 |
| Survey Altitude (AGL) | 900 m | 1,500 m |
| Target Pulse Rate | 103 – 108 kHz | 148 – 150 kHz |
| Sensor Configuration | Single Pulse in Air (SPiA) | Multiple Pulse in Air (MPiA) |
| Laser Pulse Diameter | 21 cm | 34 cm |
| Field of View | 28° | 24° |
| GPS Baselines | ≤ 13 nm | ≤ 13 nm |
| GPS PDOP | ≤ 3.0 | ≤ 3.0 |
| GPS Satellite Constellation | ≥ 6 | ≥ 6 |
| Maximum Returns | 4 | 4 |
| Intensity | 8-bit | 8-bit |
| Resolution/Density | Average 8 pulses/m ² | Average 8 pulses/m ² |
| Accuracy | RMSE _z ≤ 15 cm | RMSE _z ≤ 15 cm |

All areas were surveyed with an opposing flight line side-lap of $\geq 50\%$ ($\geq 100\%$ overlap) in order to reduce laser shadowing and increase surface laser painting. To accurately solve for laser point position (geographic coordinates x, y and z), the positional coordinates of the airborne sensor and the attitude of the aircraft were recorded continuously throughout the LiDAR data collection mission. Position of the aircraft was measured twice per second (2 Hz) by an onboard differential GPS unit, and aircraft attitude was measured 200 times per second (200 Hz) as pitch, roll and yaw (heading) from an onboard inertial measurement unit (IMU). To allow for post-processing correction and calibration, aircraft and sensor position and attitude data are indexed by GPS time.

A view looking west over the Oso landslide. The gridded bare earth model is colored by elevation and overlain with the vegetation LiDAR point cloud, showing displaced trees near the top of the slide.



LiDAR Data

Upon completion of data acquisition, QSI processing staff initiated a suite of automated and manual techniques to process the data into the requested deliverables. Processing tasks included GPS control computations, smoothed best estimate trajectory (SBET) calculations, kinematic corrections, calculation of laser point position, sensor and data calibration for optimal relative and absolute accuracy, and LiDAR point classification (Table 7). Processing methodologies were tailored for the landscape. Brief descriptions of these tasks are shown in Table 8.

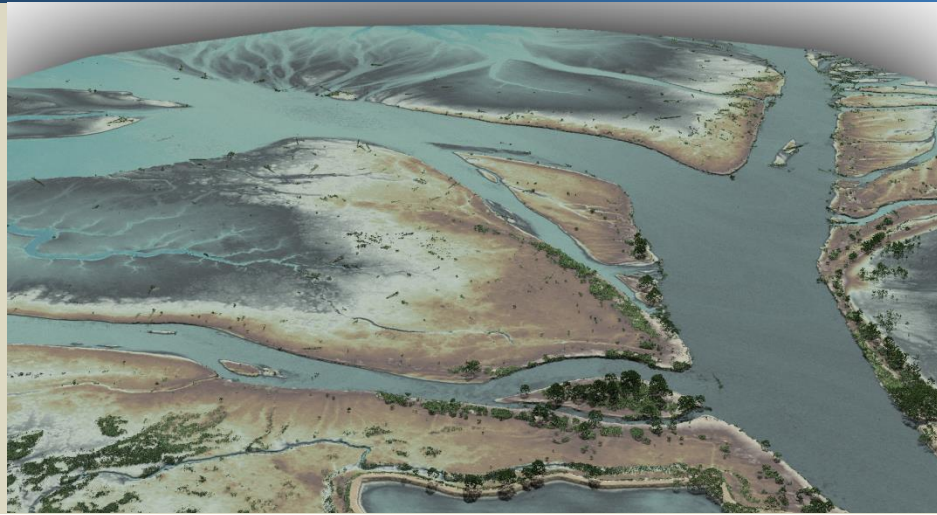
Table 7: ASPRS LAS classification standards applied to the Oso Landslide/Stillaguamish River dataset

| Classification Number | Classification Name | Classification Description |
|-----------------------|---------------------|---------------------------------------------------------------------------------------------------------------------------|
| 2 | Ground | Laser returns that are determined to be ground using automated and manual cleaning algorithms. |
| 4 | Vegetation | Vegetation. |
| 6 | Buildings | All permanent anthropogenic structures except bridges. |
| 9 | Water | Water, classified using water's edge breaklines generated using automated and manual detection and adjustment techniques. |
| 16 | Bridges | Man-made bridges. |

Table 8: LiDAR processing workflow

| LiDAR Processing Step | Software Used |
|--------------------------------------------------------------------------------------------------------------------------------------------------------------------------------------------------------------------------------------------------------------------------------------------------------------------------------------------------------------------------------------------------------------------------------------------------------------------------------------------------------------|-------------------------------------------------------|
| Resolve kinematic corrections for aircraft position data using kinematic aircraft GPS and static ground GPS data. Develop a smoothed best estimate of trajectory (SBET) file that blends post-processed aircraft position with sensor head position and attitude recorded throughout the survey. | IPAS TC v.3.1 |
| Calculate laser point position by associating SBET position to each laser point return time, scan angle, intensity, etc. Create raw laser point cloud data for the entire survey in *.las (ASPRS v. 1.2) format. Convert data to orthometric elevations by applying a geoid12a correction. | ALS Post Processing Software v.2.75 |
| Import raw laser points into manageable blocks (less than 500 MB) to perform manual relative accuracy calibration and filter erroneous points. Classify ground points for individual flight lines. | TerraScan v.14 |
| Using ground classified points per each flight line, test the relative accuracy. Perform automated line-to-line calibrations for system attitude parameters (pitch, roll, heading), mirror flex (scale) and GPS/IMU drift. Calculate calibrations on ground classified points from paired flight lines and apply results to all points in a flight line. Use every flight line for relative accuracy calibration. | TerraMatch v.14 |
| Classify resulting data to ground and other client designated ASPRS classifications (Table 7). Develop water boundary polygons using an algorithm which weighs LiDAR-derived slopes, intensities and return densities to detect the water edge. Manually review and edit the water edge as necessary. Reclassify ground classified points falling within the water polygons as water. Assess statistical absolute accuracy via direct comparisons of ground classified points to ground control survey data. | TerraScan v.14 TerraModeler v.14 Ecognition 8.9 |
| Generate bare earth models as triangulated surfaces. Generate highest hit models as a surface expression of all classified points. Export all surface models as ESRI GRIDs at a 3.0 foot pixel resolution. | TerraScan v.14 TerraModeler v.14 ArcMap v. 10.1 |
| Export intensity images as GeoTIFFs at a 1.5 foot pixel resolution. | TerraScan v.14 TerraModeler v.14 ArcMap v. 10.1 |

A view showing the mouth of the Stillaguamish River at Puget Sound. The bare earth model is colored by elevation and overlaid with the vegetation LiDAR point cloud.



LiDAR Density

The acquisition parameters were designed to acquire an average first-return density of 8 points/m² (0.74 points/ft²). First return density describes the density of pulses emitted from the laser that return at least one echo to the system. Multiple returns from a single pulse were not considered in first return density analysis. Pulse density distribution varied within the study area due to laser scan pattern and flight conditions. Additionally, some types of surfaces (e.g., breaks in terrain, water and steep slopes) may have returned fewer pulses than originally emitted by the laser. First returns typically reflect off the highest feature on the landscape within the footprint of the pulse. In forested or urban areas the highest feature could be a tree, building or power line, while in areas of unobstructed ground, the first return will be the only echo, and represents the bare earth surface.

The density of ground-classified LiDAR returns was also analyzed for this project. Terrain character, land cover, and ground surface reflectivity all influenced the density of ground surface returns. In vegetated areas, fewer pulses may penetrate the canopy, resulting in lower ground density.

The average first-return density of LiDAR data for the Oso Landslide/Stillaguamish River project was 1.28 points/ft² (13.80 points/m²) while the average ground classified density was 0.18 points/ft² (1.98 points/m²) (Table 9). The statistical and spatial distributions of first return densities and classified ground return densities per 100 m x 100 m cell are portrayed in Figure 3 through Figure 5.

Table 9: Average LiDAR point densities

| Classification | Point Density |
|-------------------|------------------------------------------------------------|
| First-Return | 1.28 points/ft ² 13.80 points/m ² |
| Ground Classified | 0.18 points/ft ² 1.98 points/m ² |

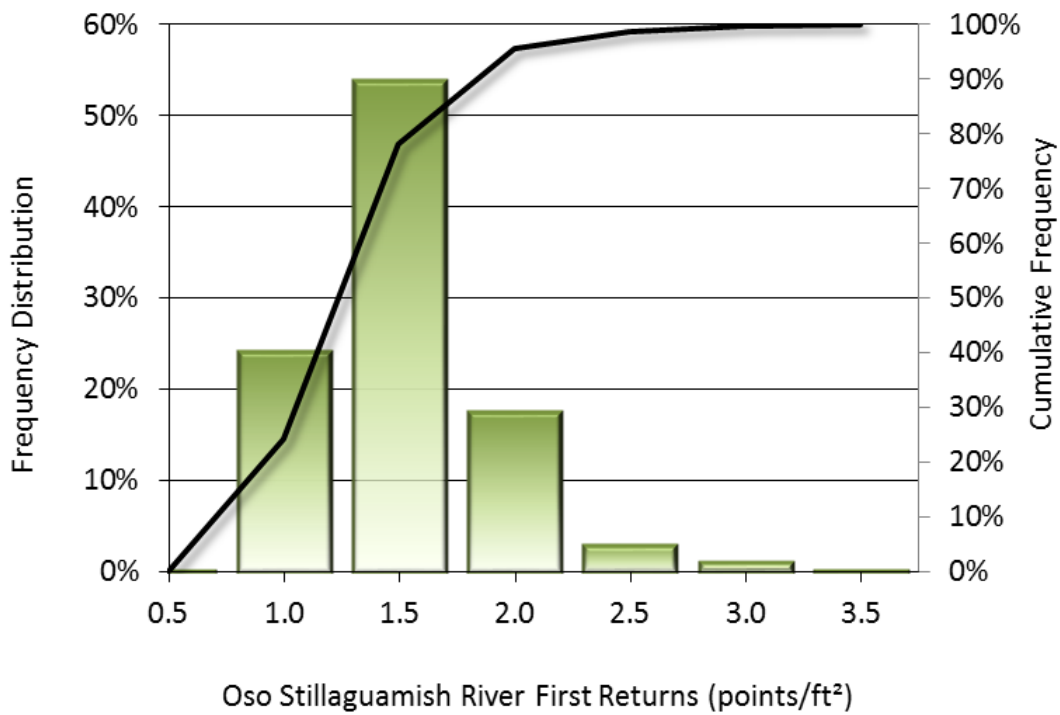


Figure 3: Frequency distribution of first return densities per 100 by 100 m cell

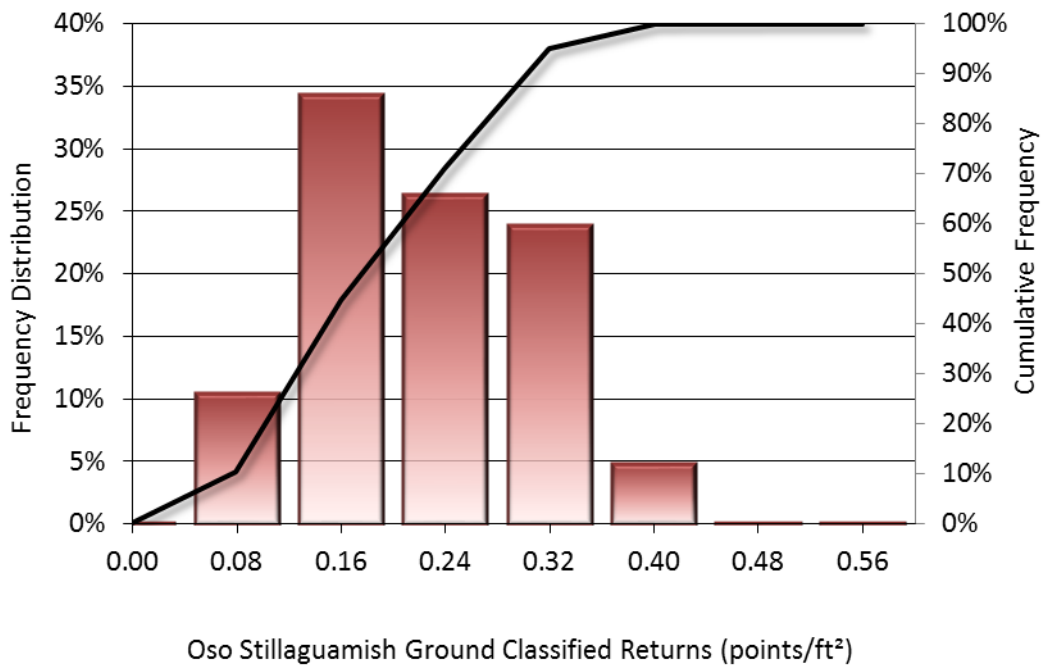


Figure 4: Frequency distribution of ground return densities per 100 by 100 m cell

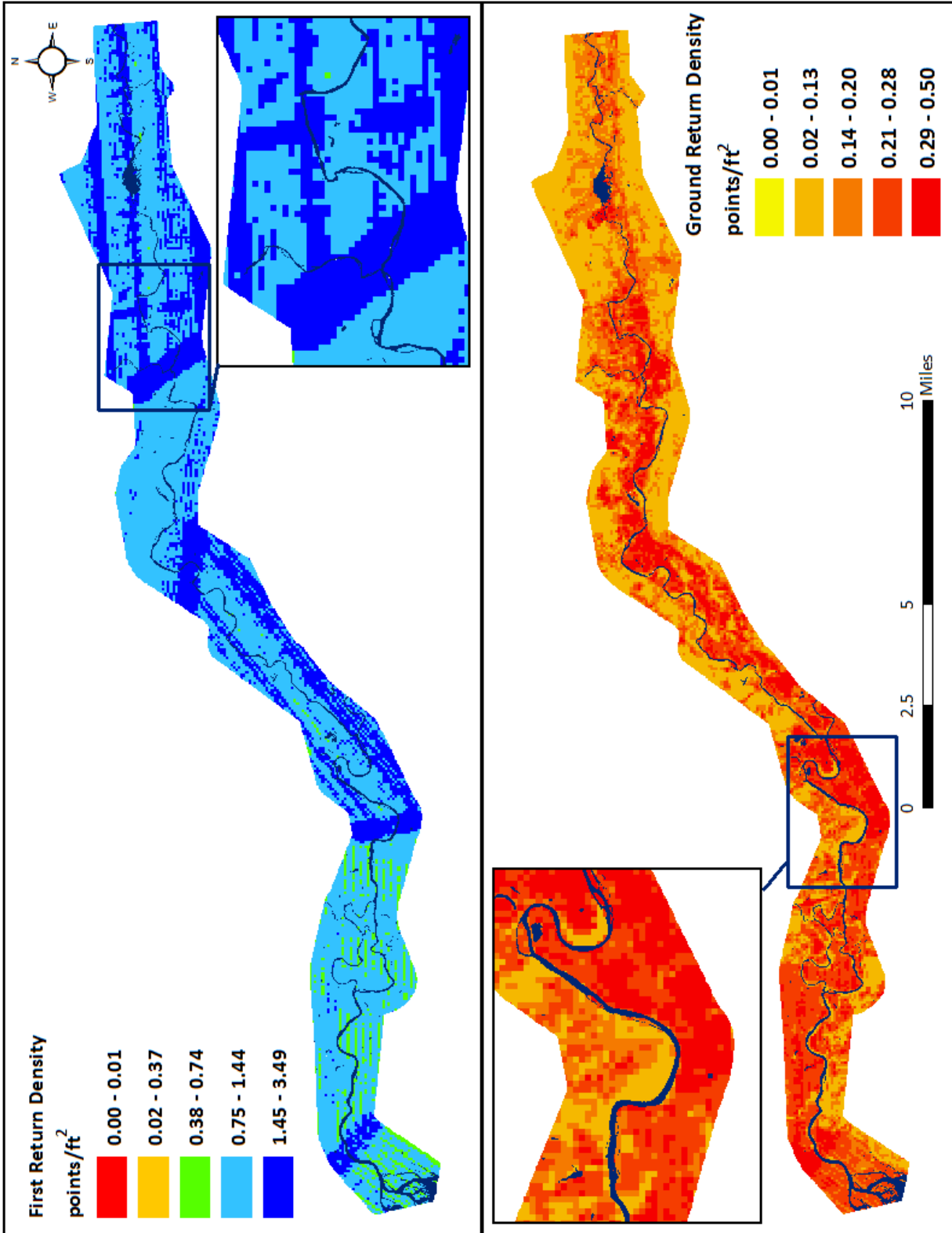


Figure 5: First return and ground density map for the Oso Landslide/Stillaguamish River site

LiDAR Accuracy Assessments

The accuracy of the LiDAR data collection can be described in terms of absolute accuracy (the consistency of the data with external data sources) and relative accuracy (the consistency of the dataset with itself). See Appendix A for further information on sources of error and operational measures used to improve relative accuracy.

LiDAR Absolute Accuracy

Absolute accuracy was assessed using Fundamental Vertical Accuracy (FVA) reporting designed to meet guidelines presented in the FGDC National Standard for Spatial Data Accuracy³. FVA compares known RTK and PPK ground control point data collected on open, bare earth surfaces with level slope (<20°) to the triangulated ground surface generated by the LiDAR points. FVA is a measure of the accuracy of LiDAR point data in open areas where the LiDAR system has a high probability of measuring the ground surface and is evaluated at the 95% confidence interval (1.96 * RMSE), as shown in Table 10.

The mean and standard deviation (sigma σ) of divergence of the ground surface model from ground survey point coordinates are also considered during accuracy assessment. These statistics assume the error for x, y and z is normally distributed, and therefore the skew and kurtosis of distributions are also considered when evaluating error statistics. For the Oso Landslide/Stillaguamish River, 1,113 ground survey points were collected in total resulting in an average accuracy of -0.025 feet (-0.008 meters) (Figure 6).

Table 10: Absolute accuracy

| Absolute Accuracy | |
|----------------------------------|-----------------------|
| Sample | 1,113 points |
| FVA (1.96*RMSE) | 0.177 ft 0.054 m |
| Average | -0.025 ft -0.008 m |
| Median | -0.023 ft -0.007 m |
| RMSE | 0.090 ft 0.028 m |
| Standard Deviation (1 σ) | 0.087 ft 0.026 m |

³ Federal Geographic Data Committee, Geospatial Positioning Accuracy Standards (FGDC-STD-007.3-1998). Part 3: National Standard for Spatial Data Accuracy. <http://www.fgdc.gov/standards/projects/FGDC-standards-projects/accuracy/part3/chapter3>

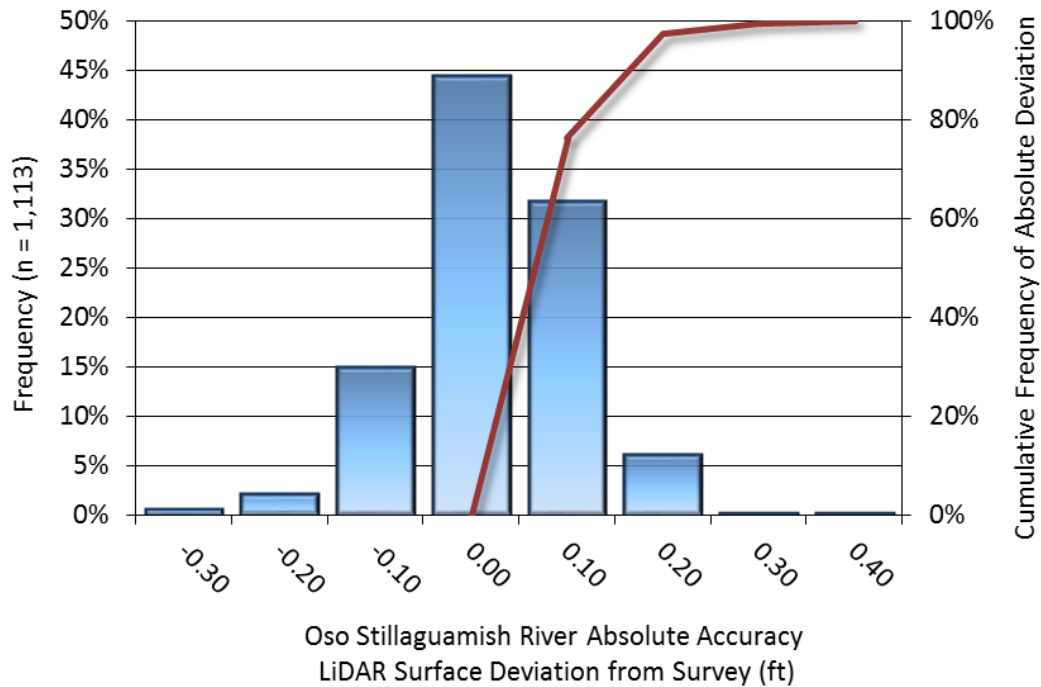


Figure 6: Frequency histogram for LiDAR surface deviation from ground survey point values

LiDAR Vertical Relative Accuracy

Relative vertical accuracy refers to the internal consistency of the data set as a whole: the ability to place an object in the same location given multiple flight lines, GPS conditions, and aircraft attitudes. When the LiDAR system is well calibrated, the swath-to-swath vertical divergence is low (<0.10 meters). The relative vertical accuracy was computed by comparing the ground surface model of each individual flight line with its neighbors in overlapping regions. The average line to line relative vertical accuracy for the Oso Landslide/Stillaguamish River project was 0.130 feet (0.040 meters) (Table 11, Figure 7).

Table 11: Relative accuracy

| Relative Accuracy | |
|-------------------------|---------------------|
| Sample | 182 surfaces |
| Average | 0.130 ft 0.040 m |
| Median | 0.128 ft 0.039 m |
| RMSE | 0.151 ft 0.046 m |
| Standard Deviation (1σ) | 0.041 ft 0.013 m |
| 1.96σ | 0.081 ft 0.025 m |

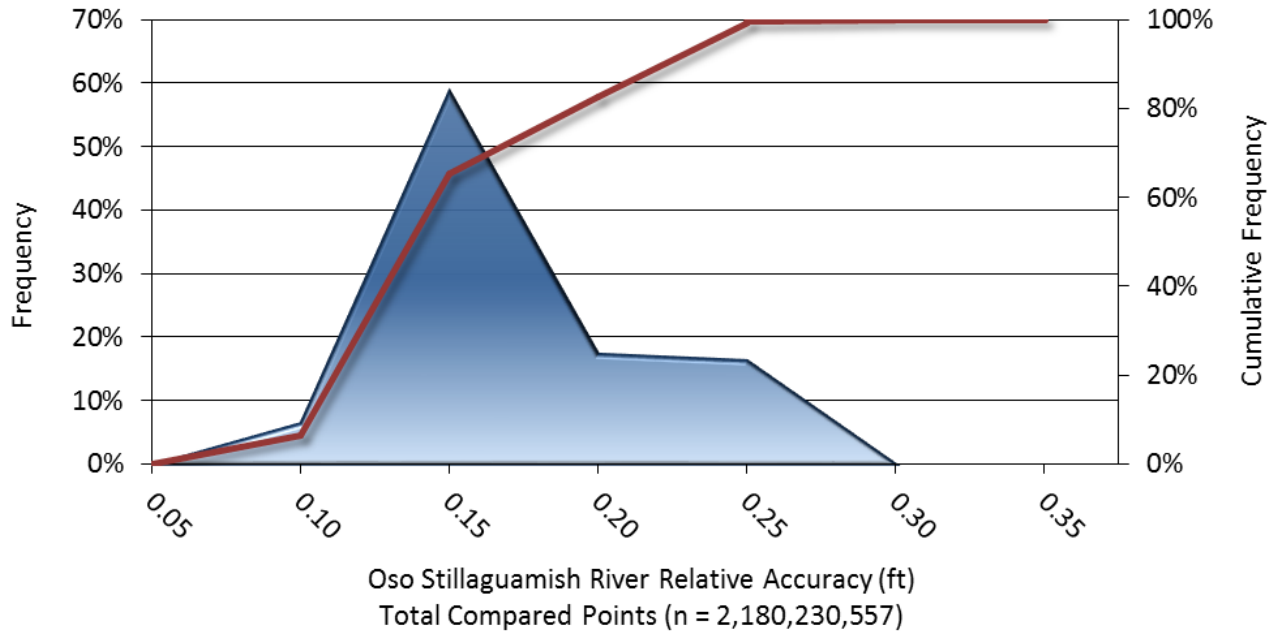


Figure 7: Frequency plot for relative vertical accuracy between flight lines

CERTIFICATIONS

Quantum Spatial provided LiDAR services for the Oso Landslide project as described in this report.

I, Kris Fausti, have reviewed the attached report for completeness and hereby state that it is a complete and accurate report of this project.



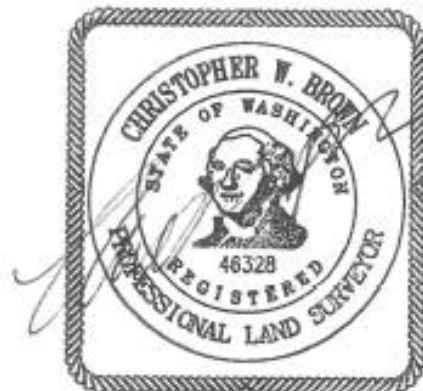
Kris Fausti
Operations Manager
WSI a Quantum Spatial Company

I, Christopher W. Brown, being duly registered as a Professional Land Surveyor in and by the state of Washington, say that I hereby certify the methodologies, LiDAR project, Static GNSS occupations on the Base Stations used during airborne flights and RTK survey on hard-surface, were performed using commonly accepted Standard Practices. Field work conducted for this report was conducted between March 24, 2014 and April 9, 2014.

Accuracy statistics shown in the Accuracy Section of this Report have been reviewed by me and found to meet the "National Standard for Spatial Data Accuracy".



Christopher W. Brown, PLS Oregon & Washington
Quantum Spatial
Portland, OR 97204



Renews: 12/21/2014

SELECTED IMAGES

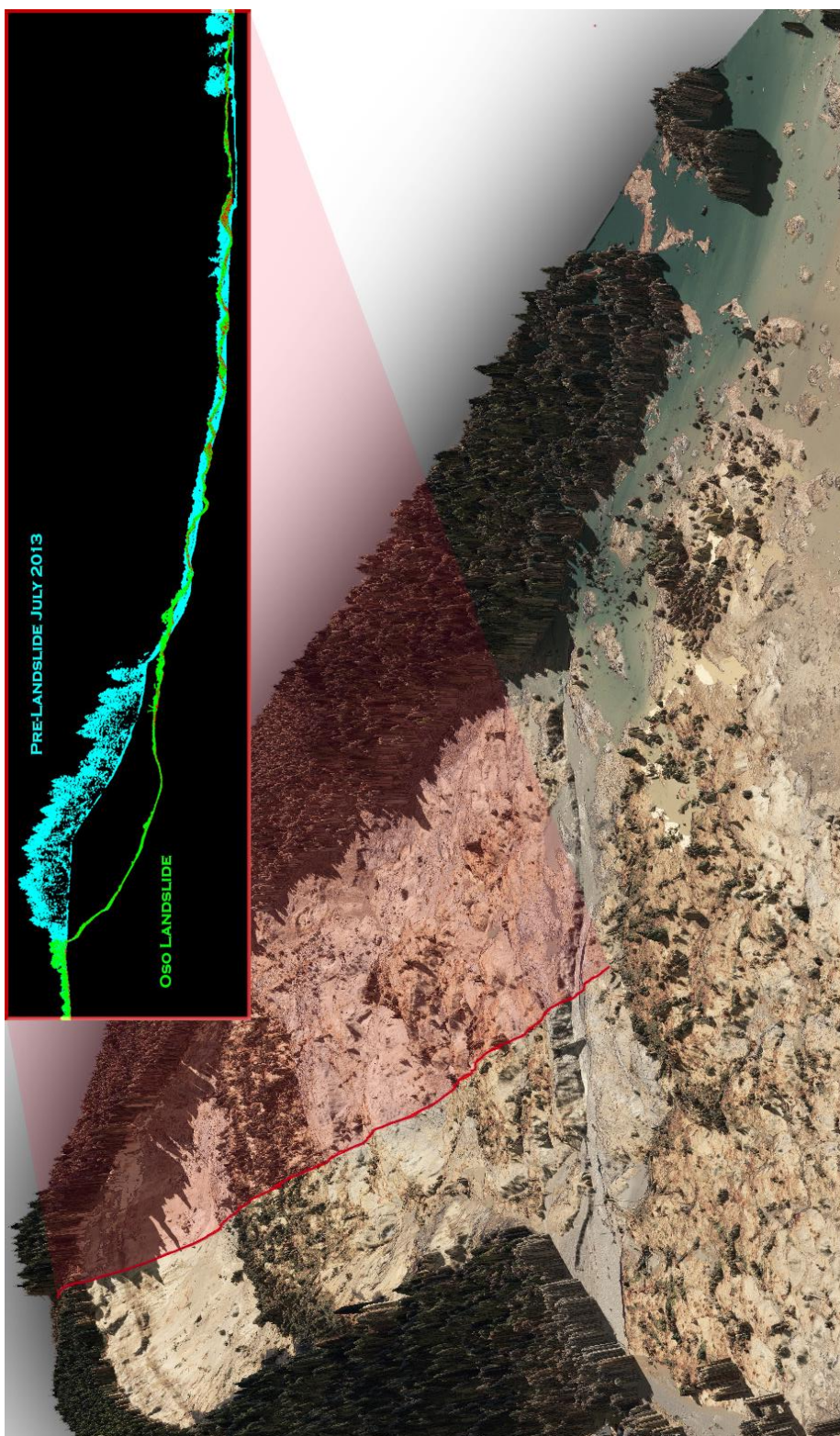


Figure 8: The Cross section shows the change in profile of the hillside from data collected in July, 2013 to just after the slide. The red line traces the cross section path along a bare earth model draped with 10 cm orthoimagery.

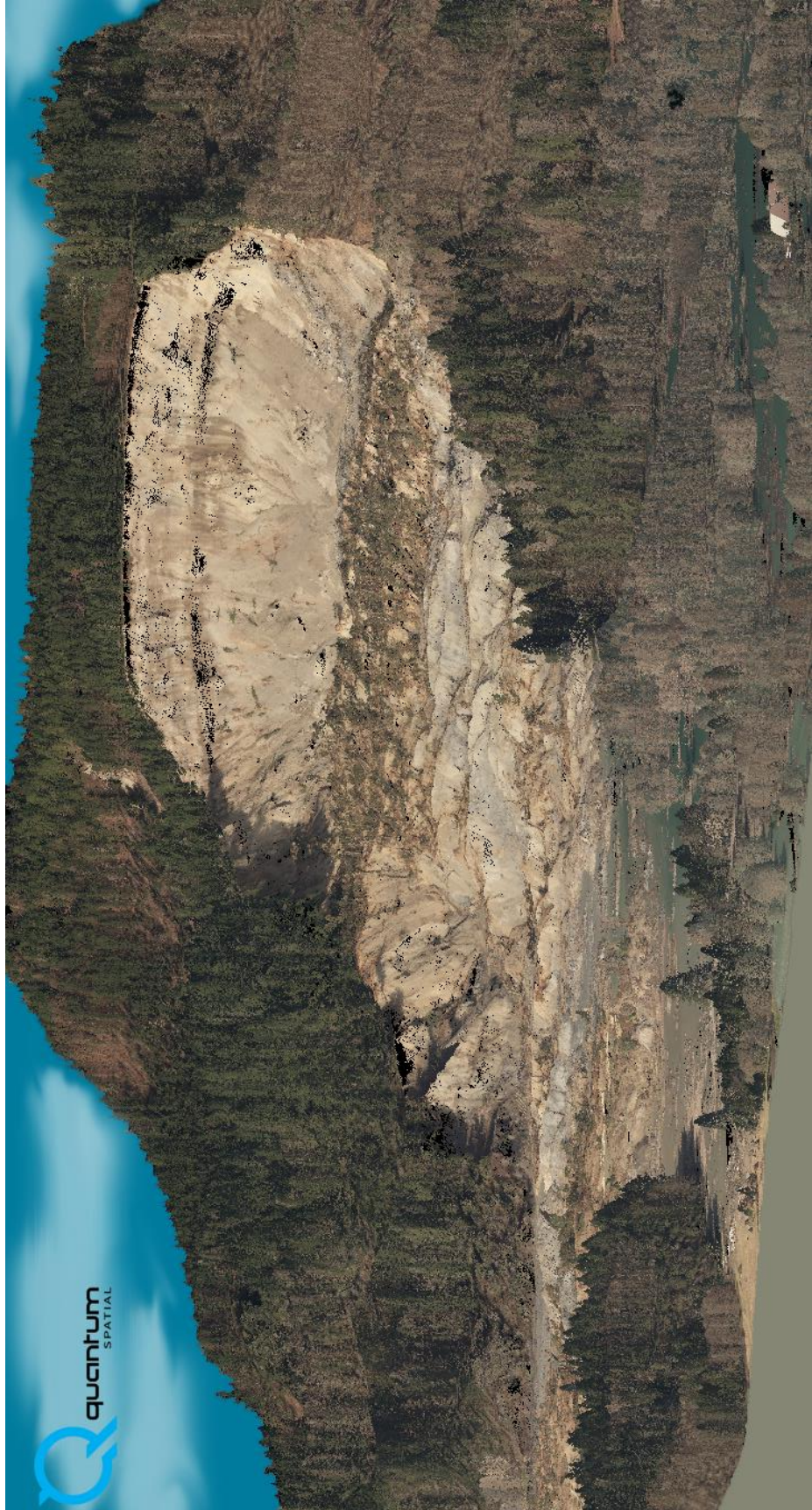


Figure 9: A 3D view of the Oso Landslide after the event in March, 2014. The processed LiDAR point cloud data are colored with aerial photography.

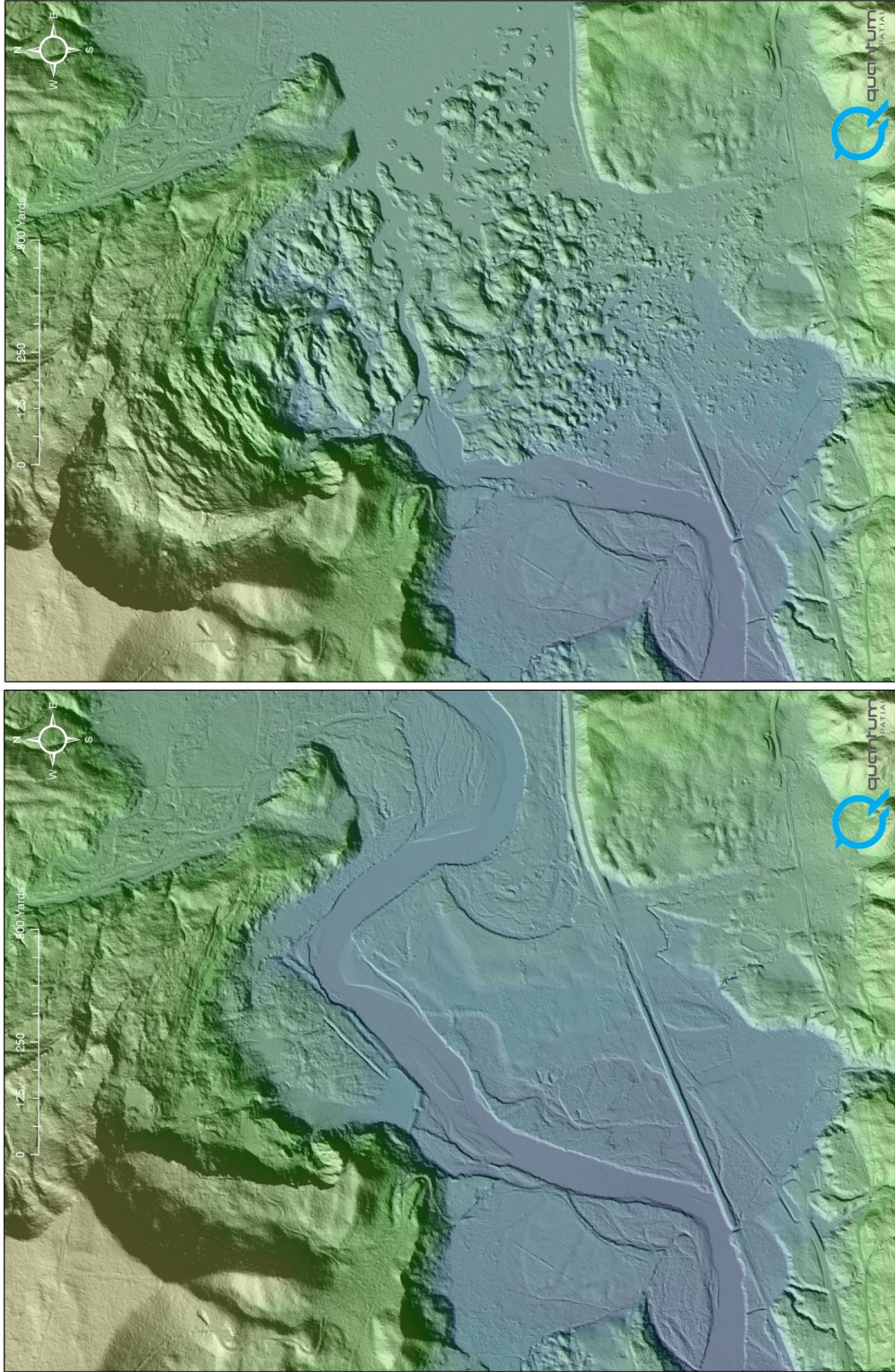


Figure 10: A view showing the shaded terrain of the Oso Landslide site before and after the event. The left image shows the site using data collected by QSI in July of 2013, and the right image shows the same view in March of 2014. The bare earth models are colored by elevation.



Figure 11: A view showing the shaded terrain of the Oso Landslide site before and after the event. The left image shows the site using data collected by QSI in July of 2013, and the right image shows the same view in March of 2014. The bare earth models are overlain with the above-ground LIDAR point cloud.

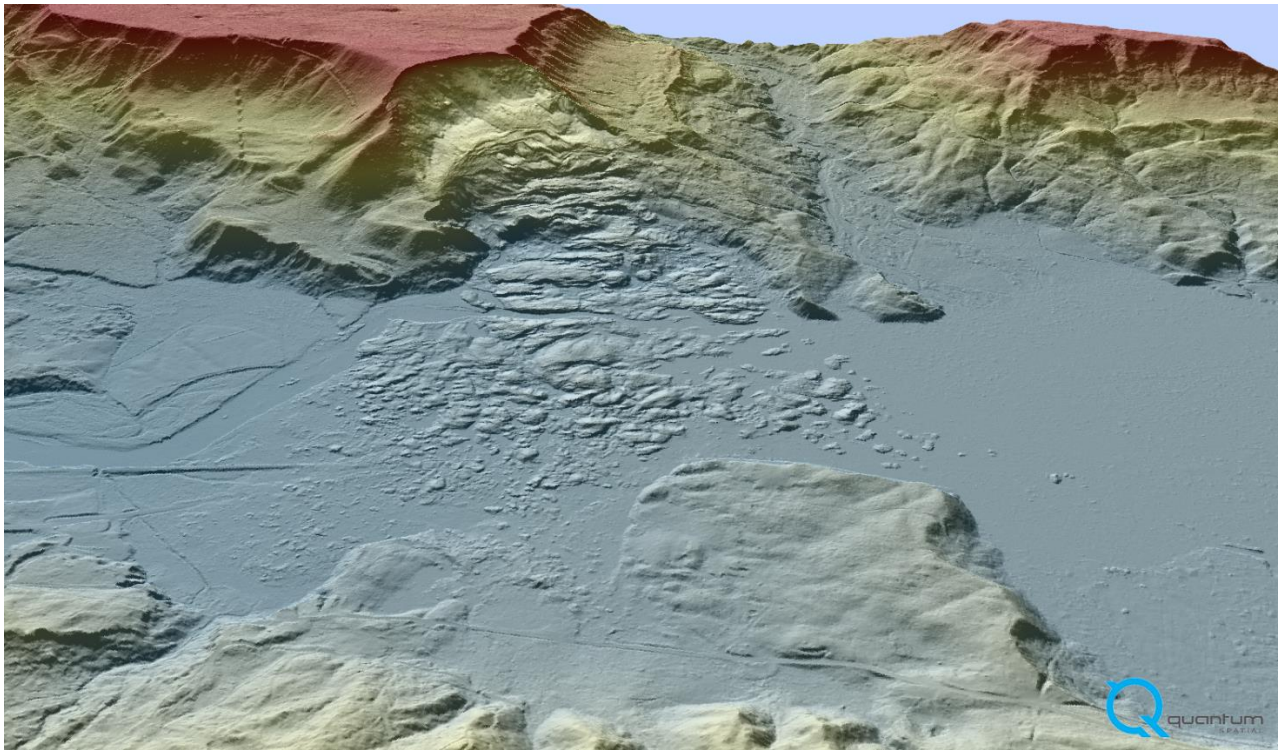
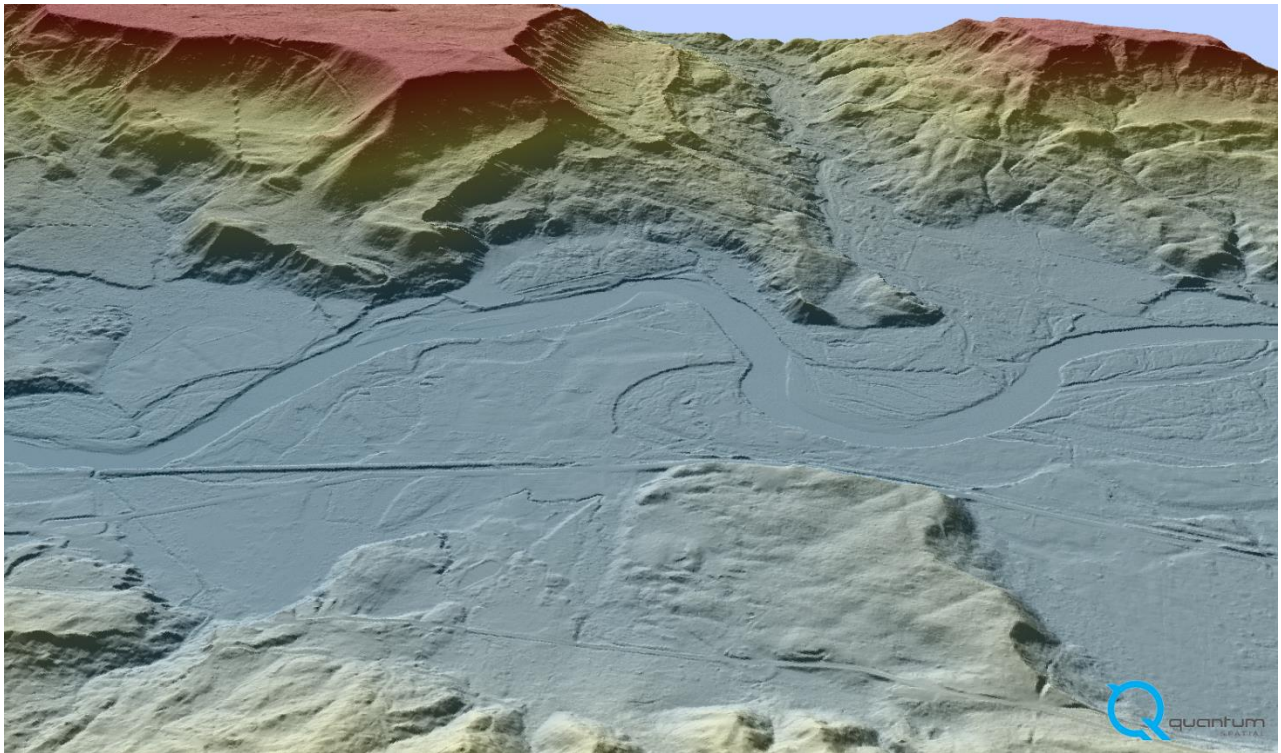


Figure 12: A 3D view showing the shaded terrain of the Oso Landslide site before and after the event. The top image shows the site using data collected by QSI in July of 2013, and the bottom image shows the same view in March of 2014. The bare earth models are colored by elevation.



Figure 13: A 3D view showing the shaded terrain of the Oso Landslide site before and after the event. The top image shows the site using data collected by QSI in July of 2013, and the bottom image shows the same view in March of 2014. The bare earth models are overlain with the above-ground LiDAR point cloud.

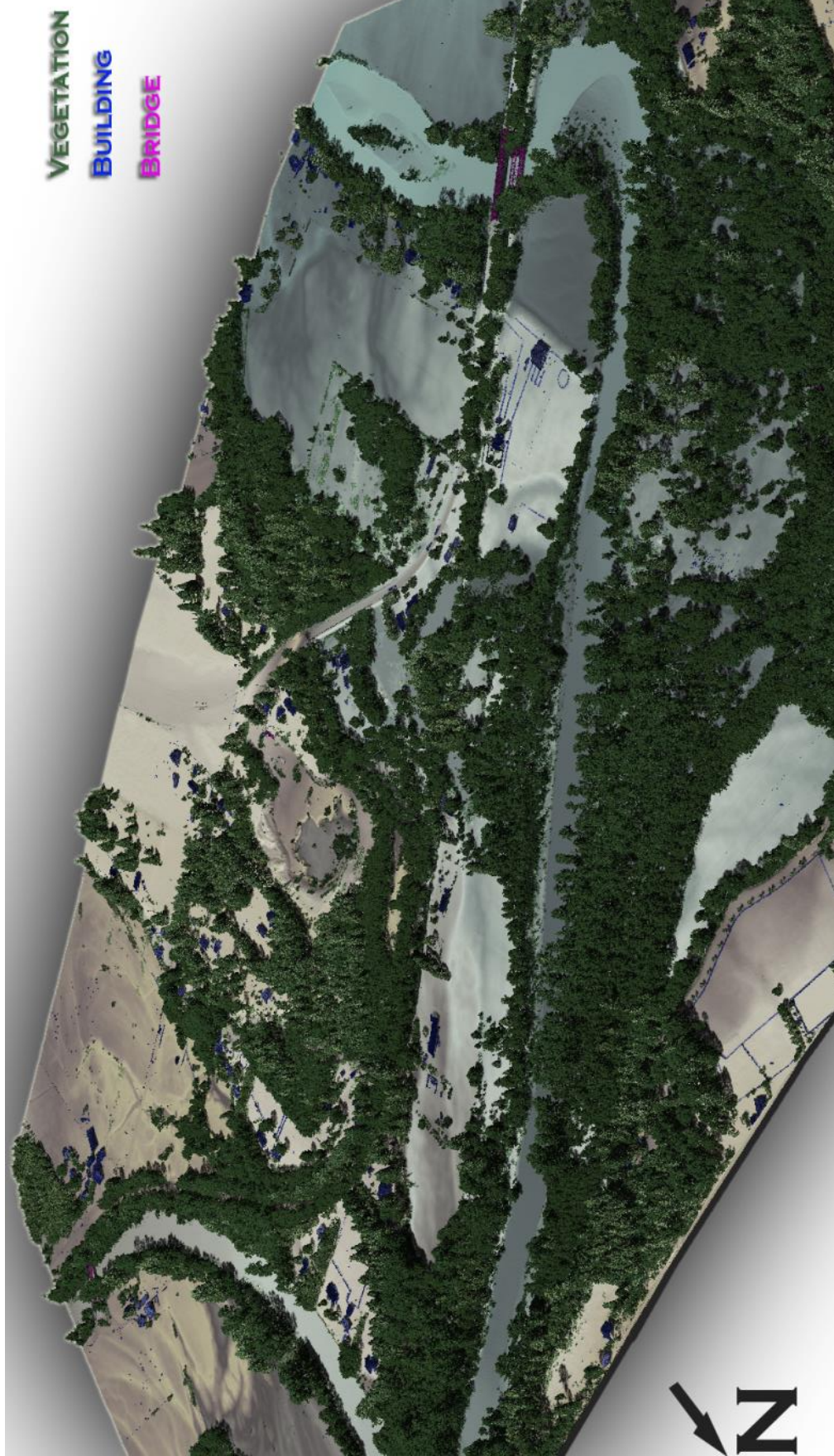


Figure 14: A view of the North Fork Stillaguamish River in the Oso Landslide/Stillaguamish River survey area. The bare earth model is colored by elevation and overlain with the classified LiDAR point cloud.

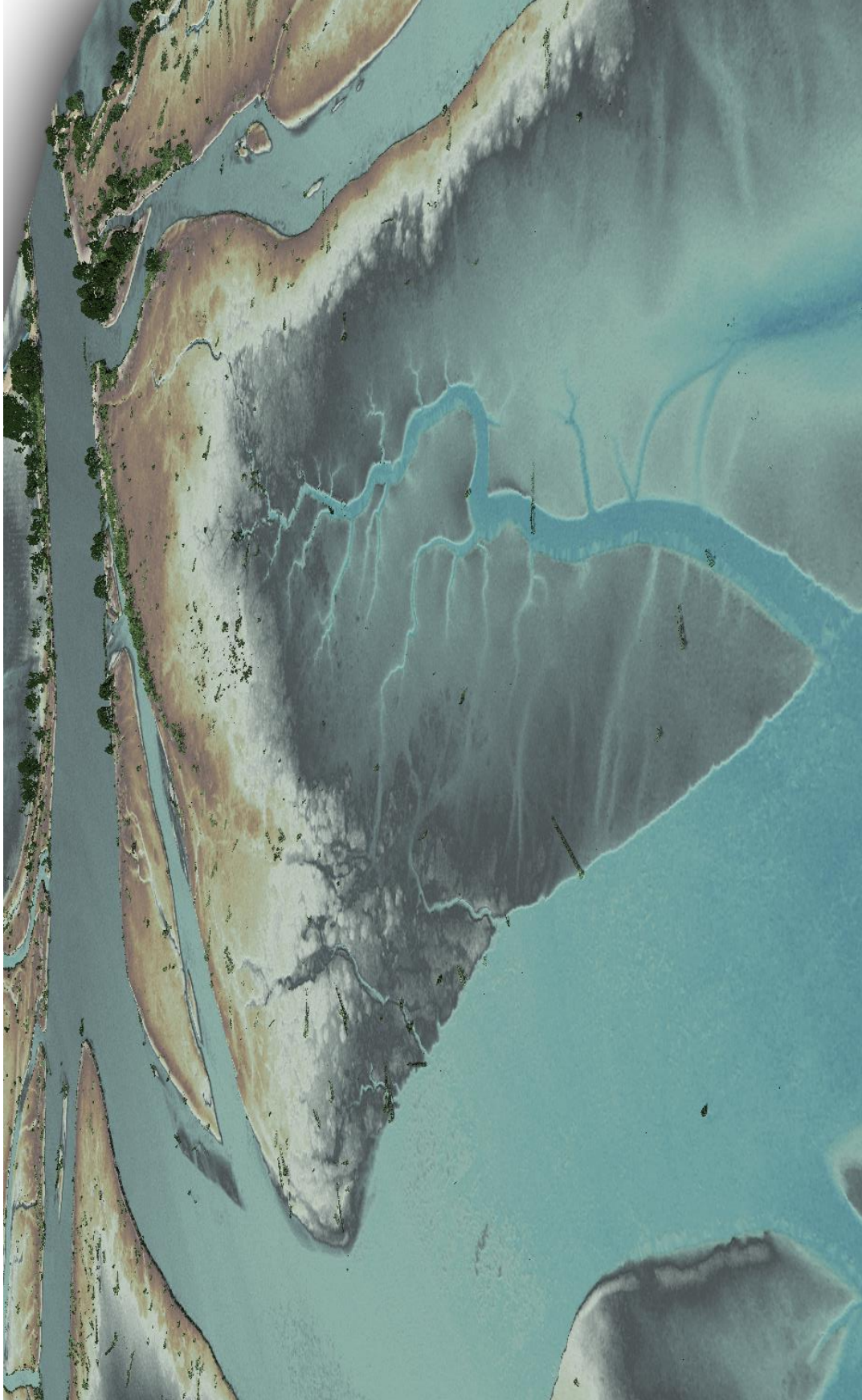


Figure 15: A view of the mouth of the Stillaguamish River at Puget Sound. The bare earth model is colored by elevation and overlain with the vegetation LIDAR point cloud.

1-sigma (σ) Absolute Deviation: Value for which the data are within one standard deviation (approximately 68th percentile) of a normally distributed data set.

1.96 * RMSE Absolute Deviation: Value for which the data are within two standard deviations (approximately 95th percentile) of a normally distributed data set, based on the FGDC standards for Fundamental Vertical Accuracy (FVA) reporting.

Accuracy: The statistical comparison between known (surveyed) points and laser points. Typically measured as the standard deviation (σ) and root mean square error (RMSE).

Absolute Accuracy: The vertical accuracy of LiDAR data is described as the mean and standard deviation (σ) of divergence of LiDAR point coordinates from ground survey point coordinates. To provide a sense of the model predictive power of the dataset, the root mean square error (RMSE) for vertical accuracy is also provided. These statistics assume the error distributions for x, y and z are normally distributed, and thus we also consider the skew and kurtosis of distributions when evaluating error statistics.

Relative Accuracy: Relative accuracy refers to the internal consistency of the data set; i.e., the ability to place a laser point in the same location over multiple flight lines, GPS conditions and aircraft attitudes. Affected by system attitude offsets, scale and GPS/IMU drift, internal consistency is measured as the divergence between points from different flight lines within an overlapping area. Divergence is most apparent when flight lines are opposing. When the LiDAR system is well calibrated, the line-to-line divergence is low (<10 cm).

Root Mean Square Error (RMSE): A statistic used to approximate the difference between real-world points and the LiDAR points. It is calculated by squaring all the values, then taking the average of the squares and taking the square root of the average.

Data Density: A common measure of LiDAR resolution, measured as points per square meter.

Digital Elevation Model (DEM): File or database made from surveyed points, containing elevation points over a contiguous area. Digital terrain models (DTM) and digital surface models (DSM) are types of DEMs. DTMs consist solely of the bare earth surface (ground points), while DSMs include information about all surfaces, including vegetation and man-made structures.

Intensity Values: The peak power ratio of the laser return to the emitted laser, calculated as a function of surface reflectivity.

Nadir: A single point or locus of points on the surface of the earth directly below a sensor as it progresses along its flight line.

Overlap: The area shared between flight lines, typically measured in percent. 100% overlap is essential to ensure complete coverage and reduce laser shadows.

Pulse Rate (PR): The rate at which laser pulses are emitted from the sensor; typically measured in thousands of pulses per second (kHz).

Pulse Returns: For every laser pulse emitted, the number of wave forms (i.e., echos) reflected back to the sensor. Portions of the wave form that return first are the highest element in multi-tiered surfaces such as vegetation. Portions of the wave form that return last are the lowest element in multi-tiered surfaces.

Real-Time Kinematic (RTK) Survey: A type of surveying conducted with a GPS base station deployed over a known monument with a radio connection to a GPS rover. Both the base station and rover receive differential GPS data and the baseline correction is solved between the two. This type of ground survey is accurate to 1.5 cm or less.

Post-Processed Kinematic (PPK) Survey: GPS surveying is conducted with a GPS rover collecting concurrently with a GPS base station set up over a known monument. Differential corrections and precisions for the GNSS baselines are computed and applied after the fact during processing. This type of ground survey is accurate to 1.5 cm or less.

Scan Angle: The angle from nadir to the edge of the scan, measured in degrees. Laser point accuracy typically decreases as scan angles increase.

Native LiDAR Density: The number of pulses emitted by the LiDAR system, commonly expressed as pulses per square meter.

APPENDIX A - ACCURACY CONTROLS

Relative Accuracy Calibration Methodology:

Manual System Calibration: Calibration procedures for each mission require solving geometric relationships that relate measured swath-to-swath deviations to misalignments of system attitude parameters. Corrected scale, pitch, roll and heading offsets were calculated and applied to resolve misalignments. The raw divergence between lines was computed after the manual calibration was completed and reported for each survey area.

Automated Attitude Calibration: All data were tested and calibrated using TerraMatch automated sampling routines. Ground points were classified for each individual flight line and used for line-to-line testing. System misalignment offsets (pitch, roll and heading) and scale were solved for each individual mission and applied to respective mission datasets. The data from each mission were then blended when imported together to form the entire area of interest.

Automated Z Calibration: Ground points per line were used to calculate the vertical divergence between lines caused by vertical GPS drift. Automated Z calibration was the final step employed for relative accuracy calibration.

LiDAR accuracy error sources and solutions:

| Type of Error | Source | Post Processing Solution |
|---------------------------|------------------------------|---------------------------------------------|
| GPS (Static/Kinematic) | Long Base Lines | None |
| | Poor Satellite Constellation | None |
| | Poor Antenna Visibility | Reduce Visibility Mask |
| Relative Accuracy | Poor System Calibration | Recalibrate IMU and sensor offsets/settings |
| | Inaccurate System | None |
| Laser Noise | Poor Laser Timing | None |
| | Poor Laser Reception | None |
| | Poor Laser Power | None |
| | Irregular Laser Shape | None |

Operational measures taken to improve relative accuracy:

Low Flight Altitude: Terrain following was employed to maintain a constant above ground level (AGL). Laser horizontal errors are a function of flight altitude above ground (about 1/3000th AGL flight altitude).

Focus Laser Power at narrow beam footprint: A laser return must be received by the system above a power threshold to accurately record a measurement. The strength of the laser return (i.e., intensity) is a function of laser emission power, laser footprint, flight altitude and the reflectivity of the target. While surface reflectivity cannot be controlled, laser power can be increased and low flight altitudes can be maintained.

Reduced Scan Angle: Edge-of-scan data can become inaccurate. The scan angle was reduced to a maximum of $\pm 15^\circ$ from nadir, creating a narrow swath width and greatly reducing laser shadows from trees and buildings.

Quality GPS: Flights took place during optimal GPS conditions (e.g., 6 or more satellites and PDOP [Position Dilution of Precision] less than 3.0). Before each flight, the PDOP was determined for the survey day. During all flight times, a dual frequency DGPS base station recording at 1 second epochs was utilized and a maximum baseline length between the aircraft and the control points was less than 13 nm at all times.

Ground Survey: Ground survey point accuracy (<1.5 cm RMSE) occurs during optimal PDOP ranges and targets a minimal baseline distance of 4 miles between GPS rover and base. Robust statistics are, in part, a function of sample size (n) and distribution. Ground survey points are distributed to the extent possible throughout multiple flight lines and across the survey area.

50% Side-Lap (100% Overlap): Overlapping areas are optimized for relative accuracy testing. Laser shadowing is minimized to help increase target acquisition from multiple scan angles. Ideally, with a 50% side-lap, the nadir portion of one flight line coincides with the swath edge portion of overlapping flight lines. A minimum of 50% side-lap with terrain-followed acquisition prevents data gaps.

Opposing Flight Lines: All overlapping flight lines have opposing directions. Pitch, roll and heading errors are amplified by a factor of two relative to the adjacent flight line(s), making misalignments easier to detect and resolve.